15th World Congress on Computational Mechanics (WCCM-XV)
8th Asian Pacific Congress on Computational Mechanics (APCOM-VIII)
Virtual Congress: 31 July – 5 August 2022
S. Koshizuka (Ed.)

ACTUATION OF CONCRETE SLABS UNDER BENDING WITH INTEGRATED FLUIDIC ACTUATORS

MARKUS NITZLADER[1], MATTHIAS J. BOSCH[2], HANSGEORG BINZ[2], MATTHIAS KREIMEYER[2] AND LUCIO BLANDINI[1]

[1] Institute for Lightweight Structures and Conceptual Design (ILEK)
University of Stuttgart
Pfaffenwaldring 14, 70569 Stuttgart, Germany
email: markus.nitzlader@ilek.uni-stuttgart.de, www.ilek.iuni-stuttgart.de

[2] Institute for Engineering Design and Industrial Design (IKTD)
University of Stuttgart
Pfaffenwaldring 9, 70569 Stuttgart, Germany
email: matthias.bosch@iktd.uni-stuttgart.de, www.iktd.uni-stuttgart.de

Key words: adaptive structures, slabs, integrated actuators, Multi-axial load transfer

Abstract. *Previous studies have shown that 33 % to 44 % of the mass embodied in residential and office buildings and up to 50 % in high-rise buildings is attributable to floor slabs. Floor slabs are typically bearing a bending load. Load-transfer through bending is not efficient because the material in the proximity of the neutral plane is practically unloaded thus resulting in a poor material utilization rate. Since bending stiffness is per se significantly lower than axial stiffness, the design of floor slabs is typically governed by deflection limits under out-of-plane loading, which causes significant oversizing. In addition, structures are typically oversized since they are designed to take extreme loading events, which in practice occur only for a small part of the service life. The ongoing climate crisis, the expected world population growth and associated resource scarcity call for new methods and solutions to build material-efficient structures that cause minimum greenhouse gas emissions. Employing adaptation strategies is a promising solution. By integrating structures with components such as sensors, actuators and control units – stress and deformation caused by live loads can be reduced actively, which enables significant material savings. Previous work carried out at the University of Stuttgart within the Collaborative Research Center 1244 has demonstrated that it is possible to compensate deflections by integrating fluidic actuators in beam structures subjected to bending. However, it is not obvious how to transfer actuation concepts employed in beams to floor slabs due to multi-axial load-transfer behaviour. In this work, fluidic actuators are strategically integrated into floor slabs to employ multi-axial transfer to counteract the effect of out-of-plane loading. This research also addresses the choice of an optimal layout of the actuators. Numerical simulations of different actuation concepts, such as uniaxial and biaxial actuation have been carried out to derive influence surfaces. The relationship between principal moments and the effect of actuation is quantified numerically. Examples are provided to show how influence surfaces can be employed to select suitable actuation strategies. Results show that displacements can be efficiently compensated through a combination of uniaxial and biaxial actuation.*

1 INTRODUCTION

1.1 The role of concrete slabs in the construction sector

The construction industry is responsible for 40 % to 50 % of global greenhouse gas emissions, more than 35 % of global energy consumption and approximately 60 % of material resource consumption [1,2]. Feasible solutions for reducing greenhouse gas emissions and material resource consumption are critical for the future sustainable development of the built environment. The life-cycle energy consumption and associated emissions for a building are made attributable to several factors. A large part of the total energy consumption is required for material production and construction stages and thus are embodied shares [3]. The embodied energy is determined by the amount and type of resources used to fabricate components and construct the building. Generally, a reduction of the building material mass yields a significant saving in the emissions associated with sourcing, transport and fabrication [4].

Floor slabs contribute significantly to the total mass of building structures. An analysis of the structural mass was carried out using data records taken from "*Baukosten Informationszentrum*" (BKI) [5]. This work considers the categorisation given in [5] which includes: office buildings, one- and two-family houses, apartment buildings, commercial buildings for manufacturing and commercial buildings for trade and storage. All load-bearing components were analysed concerning the materials used for the construction of the building. The percentage of the respective material for the load-bearing components was calculated for each of the 256 reference buildings. The calculation was carried out accounting for volume, area and length dimensions of the load-bearing components in relation to the total mass of the structures (sum of all load-bearing components). Figure 1 shows results of the analysis for shallow foundations, deep foundations, exterior walls, interior walls, interior columns, roofing and floor slabs. Results show that 33 % to 44 % of the structural mass in residential and office buildings is attributable to floor slabs. According to [6] the percentage increases up to 50 % for high-rise buildings.

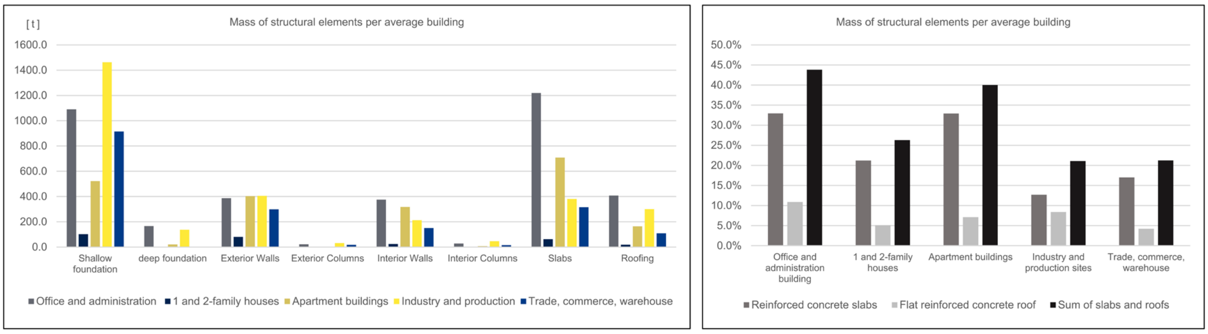

Figure 1: Mass of structural elements in buildings

Floor slabs are primarily loaded through bending. The material utilisation for bending stressed components is typically low, as the area in the proximity of the neutral plane is practically unloaded. According to [7] slab sizing is mostly stiffness governed. It is necessary to satisfy deflection limits under out-of-plane loading to prevent damage to adjacent structural and non-structural components. In addition, usually, structures are designed to take extreme loading events to satisfy safety requirements. For example, meeting rooms in office buildings must be designed for full occupancy. The same applies to slabs in multi-storey car parks. In practice, full occupancy occurs rarely and for a small part of the service time. Material savings and thus weight reductions of reinforced concrete slabs can also have a positive effect on the sizing of other components, such as columns and foundations.

Adaptation to loading through active control of stress and deflections is a promising approach for reducing the mass and related emissions of structural components [8]. Essential components for manipulating the load-bearing behaviour, e.g. to relieve stress peaks or reduce deformations, are sensors, actuators and control units. Employing such components strategically enables significant material savings [9–11]. Previous work has shown that adaptation offers great potential for material savings for stiffness governed structures [12,13].

1.2 Adaptation through integrated fluidic actuators

In the context of the Collaborative Research Centre (SFB) 1244 Adaptive Skins and Structures for the Built Environment of Tomorrow at the University of Stuttgart, new types of beam and slab components have been developed that react to loading through fluidic actuators embedded in the cross-section [14,15]. In previous work, primarily adaptive structures were developed in which truss elements were integrated with linear actuators [16] or external actuators fitted at the supports of shell structures [17].

The integration of actuators into the cross-section of beams and slabs enables an accurate and local manipulation of the structural element [8]. In addition, the actuators are not visible from the outside thus causing no visual impact. To generate actuation moments, the actuator is placed in an eccentric position at a certain distance to the neutral fibre/plane. Using the example of a beam, this was realised with lens-shaped pressure chambers consisting of welded steel sheets [8,18]. When the pressure chamber expands, the internal areas within the cross-section (cf. Figure 5) that are in contact with the lens-shaped chamber, are pushed away from each other. This way pairs of compression forces are generated that, together with the lever arm from the eccentric position, result in moment pairs counteracting the moments caused by external loads. For beams, moments along the longitudinal axis are primarily relevant. Therefore, only actuation modes in the form of a uniaxial actuation have been considered so far. For two-way slabs, moments in several spatial directions must be considered including further actuation modes. Actuation modes are understood as the working direction of forces caused by pressurised regions within the cross-section of the slab. For simplicity, such regions can be thought of as a couple of surfaces, which are referred to as “actuation faces”, that move away from or towards each other through actuation. The focus of this work is on the analysis of the adaptability of reinforced concrete two-way floor slabs. New contributions offered by this work are:

- A categorisation of actuation modes for adaptive slabs with integrated fluidic actuators.
- Setting actuation modes in relation to the principal moments caused by external loads and target displacement reduction.
- A phenomenological approach to the actuator placement and control of the structural state (e.g., stress and deformation) for two-way slabs with integrated fluidic actuators.

2 LOAD TRANSFER OF TWO-WAY SLABS

Slabs are planar structures whose width and length are significantly larger than the thickness and are subjected primarily to out-of-plane loading. A multiaxial load transfer exists if the slab is supported on at least two adjacent edges and its span ratio is $l_x/l_y < 2$ [19]. In two-way slabs, the moments m_{xy} occur in addition to moments m_x and m_y. A combination of the moments m_{xy} and the shear forces v_x and v_y result in additional forces at the corners [20]. Assume a slab is subjected to a downward distributed load and supported along all edges in the vertical downward direction. This way an upward deformation will occur at the corners. Figure 2 (a) shows the effect of the moment m_{xy} and the uplifting forces caused by a uniformly distributed load. There is zero deflection along the dashed line, here one can imagine a vertical support (e.g., a joist). Assume a strip of width d_x is cut out along the slab diagonal. This strip is supported at the joist and at the corners in the vertical downward direction but it is allowed to move in the vertical upward direction. In other words, the continuous beam ends cantilever. In this configuration, the moments are the highest at mid-span. It would therefore be effective to integrate an actuator at mid-span to reduce the moments caused by the external load locally and additionally in the corners as the cantilever effect is reduced (see section 3.3).

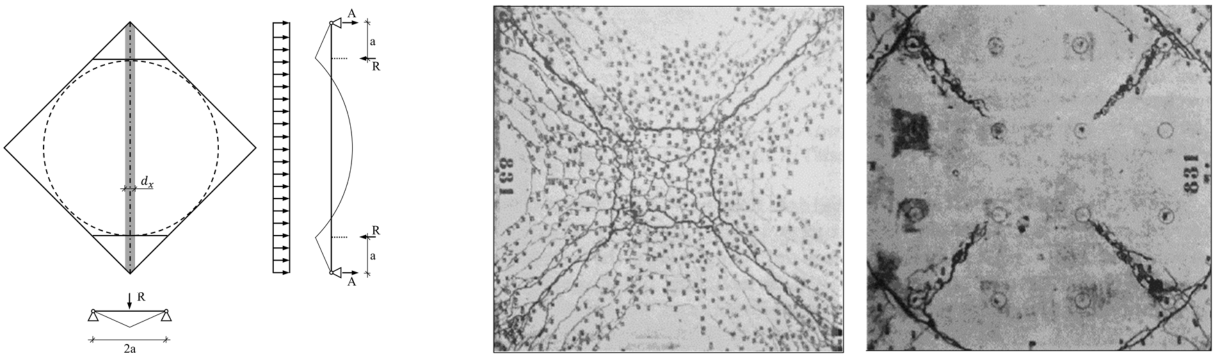

(a) (b) (c)

Figure 2: (a) Conceptual model of the load-bearing behaviour of two-way slabs, crack pattern of a simply supported two-way slab at the lower (b) and upper sides (c) [20]

Consider a typical crack pattern in a two-way slab (Figure 2 (b), (c)) subjected to a uniformly distributed load. Cracks do not develop along the direction of moments m_x and m_y. In these cases, crack propagation is also affected by the moment m_{xy} [20]. This is important concerning a possible actuation concept to counteract optimally the effect of external loads (cf. section 3.2). Cracks propagate along the principal moment (cf. Figure 3 (a)) and stress directions. As cracks are caused by extreme events, their orientation can be used to select actuation modes for reducing the effect of peak loads.

Considering the principal moment trajectories (Figure 3 (a)), the area where the moments m_1 are practically zero (no blue lines) delineates a region that has been previously referred to as a joist. In the corner regions, delimited by the joist, the sign of the principal moment m_1 changes and tensile stresses develop on the upper side of the slab corners. Actuating in this area along the tensile stresses (orthogonal to the principal moment m_1), will generate compressive forces above the neutral plane which lead to an increase in the tensile stresses and an upward deflection, increasing the effects of a uniformly distributed downward load.

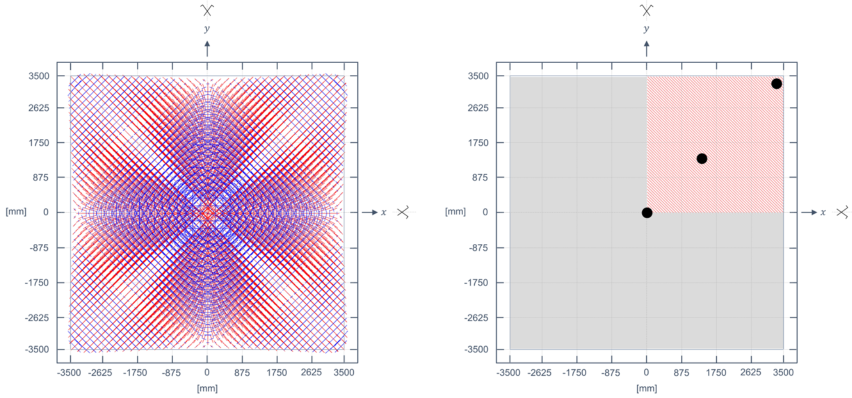

(a) (b)

Figure 3: (a) Principal moment trajectories (blue: m_1, red: m_2) under uniformly distributed load, (b) slab dimensions including selection points for Table 1.

Consider three points along one of the diagonals (figure 3 (b)) and compare the principal moments m_1 and m_2 (Table 1) caused by a uniformly distributed load. In the centre of the field, the principal moments m_1 and m_2 are equal. Further along the diagonal, m_1 is approximately half m_2. In the corner, both principal moments are approximately equal, but with opposite signs. These relations between the principal moments will be used to choose effective actuation modes to reduce the effect of the external load (cf. section 3.2).

Table 1: Excerpt of the principal moments including their ratio

Coordinates (x,y)	m_1 [kNm/m]	m_2 [kNm/m]	ratio
(0,0)	-10.8	-10.8	$m_1 = m_2$
(1450,1450)	-5.2	-10.6	$m_1 \sim ½\, m_2$
(3450,3450)	9.1	-9.1	$m_1 \sim -m_2$

3 ACTUATION MODES

3.1 Categorisation of actuation modes

Several actuation modes have been elaborated. It is possible to integrate an actuator that induces pressure in the compression zone against the stresses caused by bending. For example, this can be done through an expansion that causes two faces to move away from each other. Actuation of the tension zone requires the opposite principle. Figure 4 shows a categorisation of such actuation modes. A distinction is made as to whether forces are introduced along a line, at a point and over a wide region. Then a distinction is made as to whether compressive forces (expansion) or tensile forces (contraction) are induced in the concrete slab cross-section. In Figure 4, the direction of the induced forces is shown as a red arrow, orthogonal to the corresponding face in the cross-section (blue dashed line). Forces can be applied uniaxially, biaxially, multiaxially and omniaxially.

If there is only a cavity where an actuator is placed, it is referred to as a closed system. If the cavity is expanded and given a shape so that a concrete region is surrounded by the cavity it is referred to as an open system. If the distance between the induced pair of actuation moments is not to be limited to the cavity size, the reaction forces (yellow arrows) must be decoupled from the surrounding concrete by an appropriate actuator structure. The application of tensile forces is obtained through a combination of tension elements (e.g., cables) that work antagonistically. Since tension actuation can be developed only along a line, a large number of tension elements is required for omniaxial force application. For this reason, the categorisation is limited to uniaxial, biaxial and multiaxial. In addition to the orientation of the actuation face pairs, different intensities per axis are possible for both expansion and contraction.

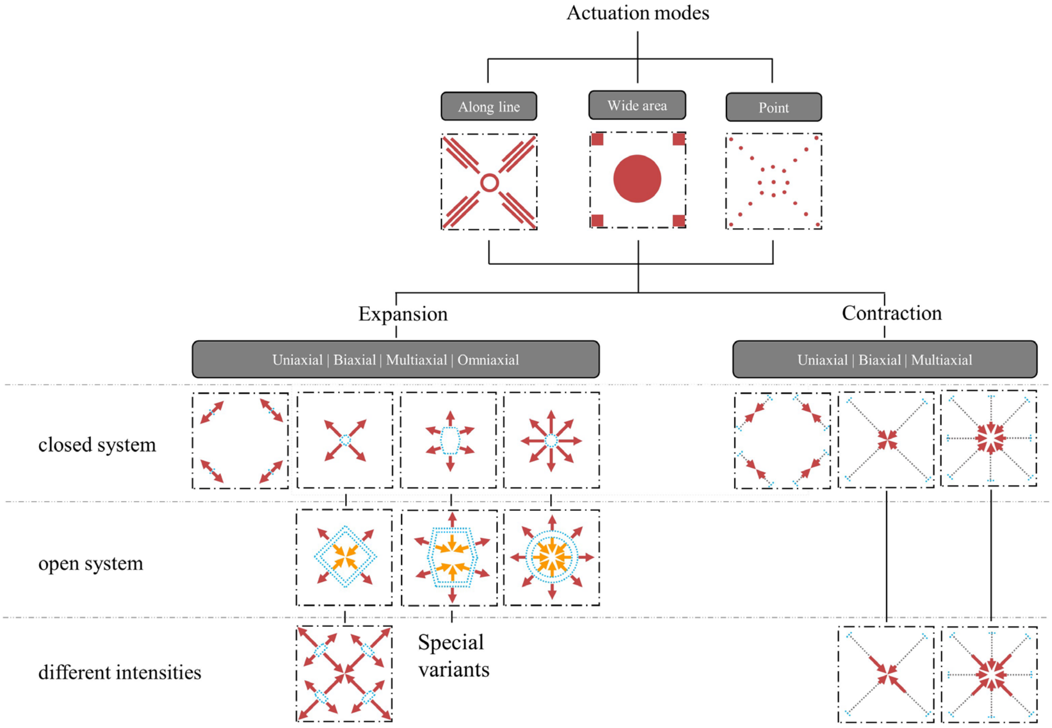

Figure 4: Categorisation of actuation modes

3.2 Relationship between actuation modes and principal moments

The ratio between the principal moments (m_1, m_2) is a useful indicator for the choice of an effective actuation mode. The purple circles in Figure 5 indicate a region in which m_1 has approximately half the magnitude of m_2. In terms of deformation control, in this region uniaxial actuation along m_1 is only half as effective as in the direction of m_2 (Figure 5 (a), (b)). A comparison of uniaxial actuation along m_2 (Figure 5 (c)) with biaxial actuation in the same region (Figure 5 (d)) shows that although the actuation face total area is identical, uniaxial actuation performs better because the orientation of the actuation forces counteract better the effect of the dominant moment m_2. Between the single cavities for the biaxial actuators, no moment can be generated in the direction of m_2 which thus cannot be reduced. The space between the five biaxial actuators was chosen following the formulation in [8]. Results and input parameters of the benchmark are given in Table 2. Since it is unfeasible to provide a continuous active region in both directions, the dominant actuation direction should have a larger actuation face.

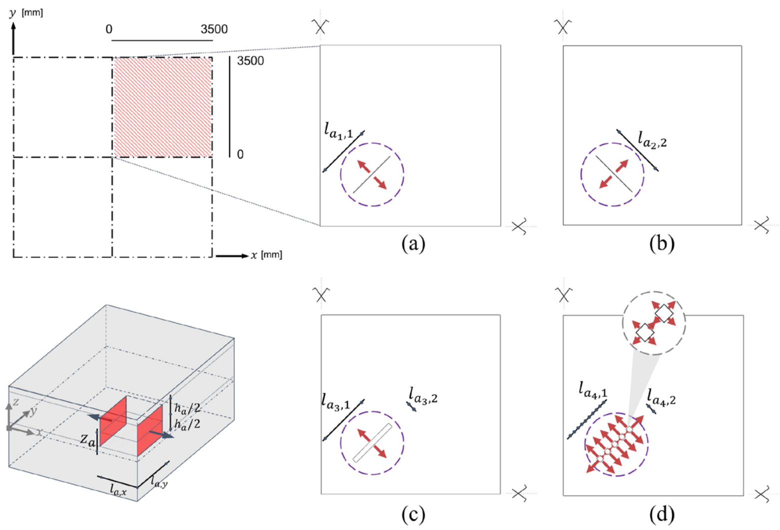

Figure 5: Comparison of actuation modes according to their relation to the principal moments. Uniaxial actuation, orientation along principal moment m_2 (a) and m_1 (b). Uniaxial actuation along principal moment m_2 with an identical total area of the actuation faces compared to biaxial actuation (d), where the orientation is along the principal moments m_1 and m_2.

The actuation moment depends on the area of the actuation faces, the lever arm and the applied pressure [8]. To keep required pressures low, biaxial actuation is preferable to omniaxial actuation, since the surface area of a prism is larger than that of a cylinder (base circle inscribed) and the principal moments can be counteracted by actuating in two directions.

Table 2: Parameters for the uniaxial/uniaxial and uniaxial/biaxial comparison

uniaxial / uniaxial						
actuation mode	face height	face length $l_{a_1,1} = l_{a_2,2}$	face length $l_{a_1,2} = l_{a_2,2}$	total face area	actuation pressure	displacement w slab midspan
uniaxial along m_1	71 mm	1.000 mm	6 mm	142.000 mm²	100 bar	0,033 mm
uniaxial along m_2	71 mm	1.000 mm	6 mm	142.000 mm²	100 bar	0,079 mm
uniaxial / biaxial						
actuation mode	face height	face length $l_{a_1,1}$; $l_{a_2,2}$	face length $l_{a_1,2} = l_{a_2,2}$	total face area	actuation pressure	displacement w slab midspan
uniaxial along m_2	71 mm	1.000 mm	100 mm	142.000 mm²	100 bar	0,193 mm
biaxial 5x	71 mm	100 mm	100 mm	142.000 mm²	100 bar	0,083 mm

Results have been obtained for a simply supported slab with both dimensions l_x and l_y set to 7 m as indicated in Figure 5, the thickness to 0.23 m, the Young's modulus to 34,000 N/mm² and the Poisson's ratio to 0.2. The span of 7 m is a common measurement for slabs of constant cross-section [21,22]. The thickness is designed for a distributed load of 5 kN/m² in the passive system state. The slab has been modelled in ABAQUS and consists of solid elements C3D10 with an approximate element size of 45 mm and 15 mm for the actuator cavities. The C3D10 element is a second-order tetrahedral element with 10 nodes and four integration points. Symmetry conditions are exploited so that only one quadrant has been modelled.

3.3 Influence surfaces

Influence surfaces for slabs offer the possibility to analyse deflections and stress resultants for variable loads and to determine the most critical load position [23]. To select effective actuation modes, in this work actuation influence matrices [24] are employed to produce influence surfaces for different actuation modes. Figure 6 shows examples of influence surfaces for a 7 x 7 m simply supported slab. Figure 6 (a_1) and (a_2) shows the influence surface of biaxial actuation and (b_1), (b_2) and (b_3) the influence surface of uniaxial actuation applied along the moment m_2. In both cases, the influence on the deflection at the slab midspan (centre point) is evaluated. Perspective and top views of the influence surfaces are shown. Referring to Figure 3 (a) and Figure 6, one can observe the connection between the external load-case independent influence of actuation on the control objective, the direction of the principal moments caused by a uniformly distributed load (cf. section 2) and the used actuation mode. The uniaxial actuation is effective if m_2 can be counteracted (along one diagonal). For the second diagonal, the actuation mode must be rotated 90° to achieve the same effect. Along the diagonal where the moment m_1 is counteracted, there is a negative influence on the midspan deflection starting if actuators are placed in the region where the moment sign changes. This is also the reason why biaxial actuation is effective in the middle of the slab and approaches zero influence beyond the region where m_1 change sign. By addressing both directions in the region of the m_1 sign change, the actuation influences cancel each other out.

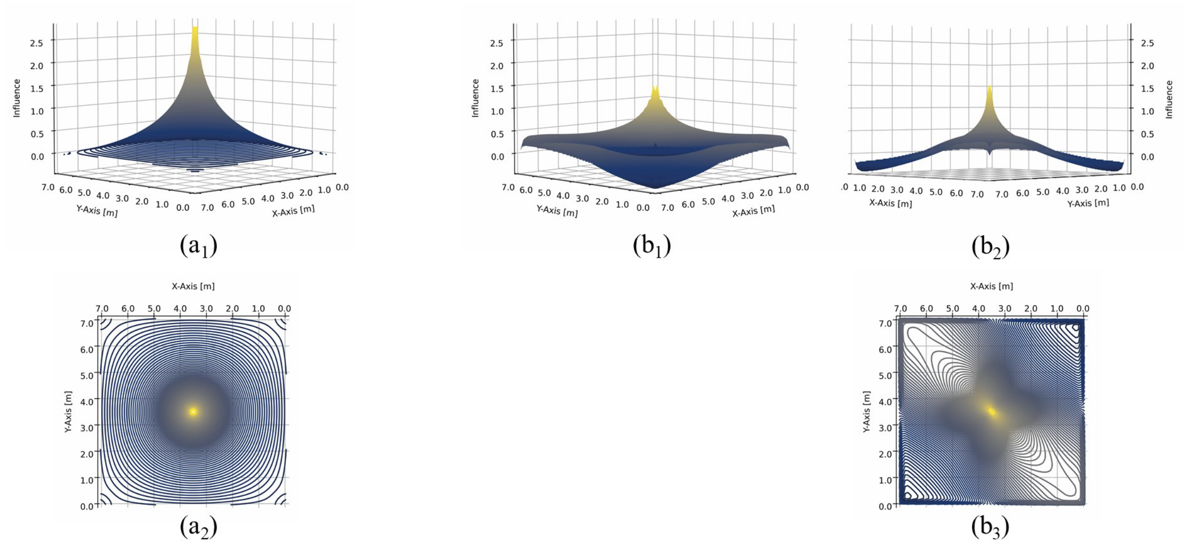

Figure 6: Influence surfaces for: (a_1) biaxial actuation mode, (a_2) top view of a biaxial actuation mode, (b_1) uniaxial actuation mode (view at the addressed diagonal), (b_2) a uniaxial actuation mode (view along the addressed diagonal), (b_3) top view of a uniaxial actuation mode

3.4 Case study

A possible actuator placement based on the described relationship between principal moments and actuation modes is shown in Figure 7 (b). All actuation regions, including the long actuation faces, correspond to the type of closed system (cf. Figure 4). In the range of

$m_1 = m_2$, actuation is exclusively biaxial. Going further up to the sign change of m_1, moment m_2 is primarily counteracted through uniaxial actuation. The same applies to m_1 using smaller actuation faces since m_2 is dominant. After the change of sign, only uniaxial actuation takes place. Overall, the actuation region is limited to the region where the principal stresses are the highest on the lower face of the slab (Figure 7 (a)). To compare the area used for actuation (XY plane), the uniaxial actuators are grouped into individual rows (indicated in different colours in Figure 7 (b)).

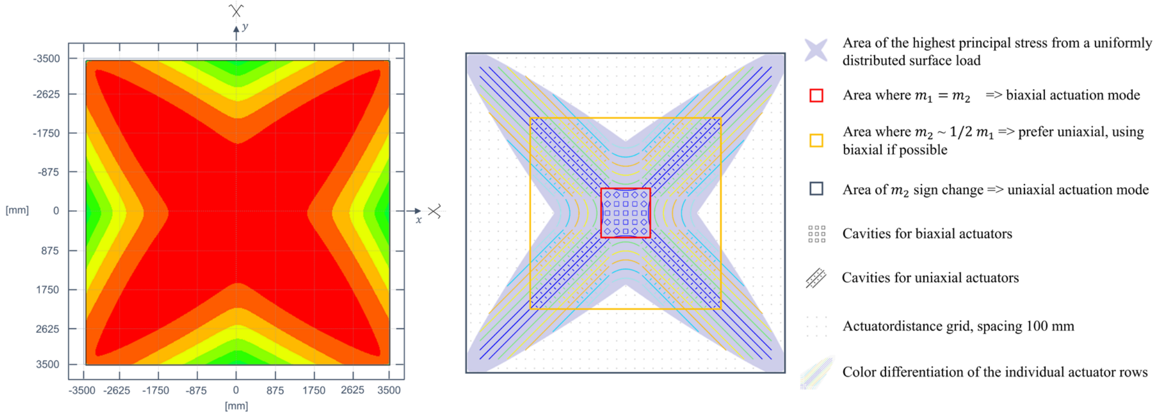

(a) (b)

Figure 7: Actuator placement

To compensate the deformations, the absolute value of the translational displacement *w* at point *P* (maximum displacement at midspan) caused by a uniformly distributed load (passive state) is related to the influence of a unit load actuation (Equation 1).

$$F_a = \frac{|w_{pas|P}|}{\sum_1^n w_{a_n|P,}} \tag{1}$$

The influences of the individual actuators can be considered individually and added up. Table 3 shows the required actuation pressure to compensate the deformations from a uniformly distributed load of 5 kN/m² for each actuator row.

Table 3: Midspan displacements in the active and passive state and actuation pressures per actuator row

Load case active = 1 N/mm² passive = 5 kN/m²	w_{active} [mm]	$w_{passive}$ [mm]	F_a [N/mm²]
Actuator row 1	0.13239	-1.48610	11.22
Actuator row 1-2	0.19298	-1.51941	7.87
Actuator row 1-3	0.24176	-1.54665	6.40
Actuator row 1-4	0.27814	-1.56650	5.63
Actuator row 1-5	0.30138	-1.57899	5.24
Actuator row 1-6	0.31064	-1,58399	5.10

The adaptive system state describes the superposition of the displacements in the passive state and the displacements caused by actuation (active state). Using the computed actuation pressure (Table 3) Figure 8 shows results for actuator row 1. The colourmap plot shows the translational displacements in the passive (Figure 8 (a)) and adaptive (Figure 8 (b)) states. In addition, the maximum principal stresses on the lower face of the slab are indicated in Figure 8 (c) for the passive state and (d) for the adaptive state.

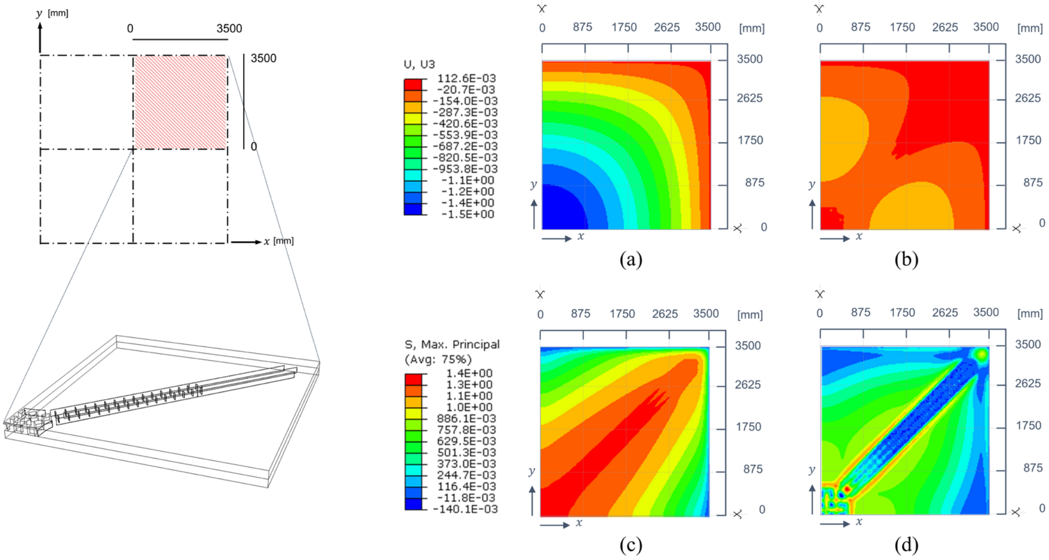

Figure 8 Results for actuator row 1: displacements in mm for passive (a) and adaptive (b) state; maximum principal stresses in N/mm² for passive (c) and adaptive (d) state at the bottom of the slab

The deformations at midspan can be completely reduced through actuator row 1 only and there is a reduction of the deformations in the rest of the slab. In addition, the maximum principal stresses can be reduced, especially in the proximity of the actuator region. If all actuator rows are used, the required pressure can be significantly reduced (Table 3) and the deformation pattern in the adaptive state becomes more homogeneous (Figure 9 (b)).

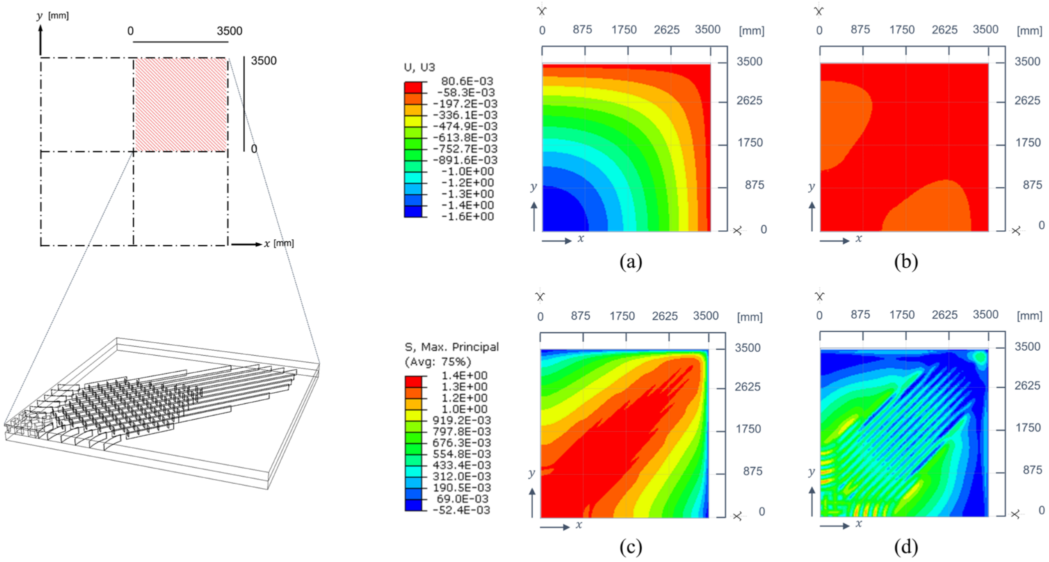

Figure 9: Results for actuator row 1-6: displacements in mm for passive (a) and adaptive (b) state; maximum principal stresses in N/mm² for passive (c) and adaptive (d) state at the bottom of the slab

4 DISCUSSION

If the actuation domains are characterized by the type of closed system (cf. Figure 4) and placed along a line in combination with point regions, a relatively large number of actuators is required. Ongoing work is looking into the type of open system (cf. Figure 4) and actuation domains that expand over a wide area with decoupling from the surrounding concrete. Through actuation influence matrices, the actuation faces can be effectively placed. Current investigations indicate that the number of actuators can be reduced by a factor of 10.

In the proximity of the slab midspan, the moment caused by a uniformly distributed load can be assumed to be constant for simplicity. Since a variation of the actuation pressure is necessary outside such an area of the constant moment, using actuator domains that expand over extended regions (along a line) has enabled applying the same pressure to all actuators. Although this is sufficient for deformation control, stresses in the corner regions cannot be effectively reduced. To determine different actuation pressures, the approach presented in [17] based on the influence matrices can be used.

5 CONCLUSIONS

It has been shown that two-way slabs require new actuation modes while taking into account the actuation domain. The principal moment ratio is a useful indicator for the choice of an effective actuation mode. The presented categorisation together with influence surfaces and actuation influence matrices provides an aid to carry out effective actuator placement.

The shown complete deformation reduction has been obtained through relatively low actuation pressures (5.10 N/mm²) which shows good potential for material mass savings, especially since floor slabs are typically stiffness governed structures.

ACKNOWLEDGMENTS

This work is funded by the Deutsche Forschungsgemeinschaft (DFG, German Research Foundation) – Project-ID 279064222 – SFB 1244. The authors are grateful for the generous support.

REFERENCES

[1] Sobek W., *Non nobis - über das Bauen in der Zukunft, Bd. 1: Ausgehen muss man von dem, was ist,* Bd. 1, av edition, Stuttgart 2022.

[2] UNEP, *2020 Global status report for buildings and construction: towards a zero-emission, efficient and resilient buildings and construction sector,* Nairobi 2020.

[3] Bechmann R., Weidner S., *Reducing the Carbon Emissions of High-Rise Structures from the Very Beginning,* „CTBUH Journal“ 2021, Issue IV, p. 30–35.

[4] Dunant C.F., Drewniok M.P., Orr J.J., Allwood J.M., *Good early stage design decisions can halve embodied CO2 and lower structural frames' cost,* „Structures“ 2021 (33), p. 343–354.

[5] BKI Kostenplaner 2021 - *Statistik plus, Positionen,* Baukosteninformationszentrum Deutscher Architektenkammern GmbH, Stuttgart 2021.

[6] Berger T., Prasser P., Reinke H.G., *Einsparung von Grauer Energie bei Hochhäusern,* „Beton- und Stahlbetonbau“ 2013, No. 6(108), p. 395–403.
[7] Zilch K., Rogge A., *Bemessung von Stahlbeton- und Spannbetonbauteilen im Brücken- und Hochbau,* „Beton-Kalender“ 2004, No. 2(93, 2), p. 281–283.
[8] Kelleter C., Burghardt T., Binz H., Blandini L., Sobek W., *Adaptive concrete beams equipped with integrated fluidic actuators,* „Frontiers in Built Environment“ 2020 (6), p. 107–119.
[9] Sobek W., *Ultra-lightweight construction,* „International Journal of Space Structures“ 2016, No. 1(31), p. 74–80.
[10] Ostertag A., *Zuverlässigkeit, Sicherheit und Nachhaltigkeit adaptiver Tragwerke,* Universität Stuttgart 2021.
[11] Wang Y., Senatore G., *Design of adaptive structures through energy minimization: extension to tensegrity,* „Structural and multidisciplinary optimization : journal of the International Society for Structural and Multidisciplinary Optimization“ 2021, No. 3(64), p. 1079–1110.
[12] Geiger F., Gade J., Scheven M. von, Bischoff M., *A case study on design and optimization of adaptive civil structures,* „Frontiers in Built Environment“ 2020 (6), p. 94.
[13] Steffen S., Blandini L., Sobek W., *Analysis of the inherent adaptivity of basic truss and beam modules by means of an extended method of influence matrices,* „Engineering Structures“ 2022, accepted for publication.
[14] Kelleter C., Sobek W., Burghardt T., Binz H., *Actuation of structural concrete elements under bending stress with integrated fluidic actuators,* [in:] A. Zingoni (ed.), *7th International Conference on Structural Engineering, Mechanics and Computation (SEMC 7), September 2-4, 2019, Cape Town, South Africa,* CRC Press, Boca Raton 2019.
[15] Sobek W., Sawodny O., Bischoff M., Blandini L., Böhm M., Haase W., Klett Y., Mahall M., Weidner S., Burghardt T., Leistner P., Maierhofer M., Park S., Reina G., Roth D., Tarín C., *Adaptive Hüllen und Strukturen,* „Bautechnik“ 2021, No. 3(98), p. 208–221.
[16] Senatore G., Duffour P., Winslow P., Wise C., *Shape control and whole-life energy assessment of an ‘infinitely stiff’ prototype adaptive structure,* „Smart Materials and Structures“ 2018, No. 1(27), p. 15022.
[17] Neuhäuser S., Weickgenannt M., Witte C., Haase W., Sawodny O., Sobek W., *Stuttgart Smartshell - a full scale prototype of an adaptive shell structure,* „Journal of the International Association for Shell and Spatial Structures“ 2013, No. 178(54), p. 259–270.
[18] Burghardt T., Kelleter C., Bosch M., Nitzlader M., Bachmann M., Binz H., Blandini L., Sobek W., *Investigations of a large-scale adaptive concrete beam with integrated fluidic actuators,* „Civil Engineering Design“ 2022 (4), accepted for publication.
[19] Zilch K., *Bemessung im konstruktiven Betonbau: Nach DIN 1045-1 (Fassung 2008) und EN 1992-1-1 (Eurocode 2),* SpringerLink Bücher, Springer Berlin Heidelberg, Berlin, Heidelberg 2010.
[20] König G., Tue N.V., *Grundlagen des Stahlbetonbaus: Einführung in die Bemessung nach DIN 1045-1,* Teubner Studienbücher Bauwesen, Vieweg+Teubner Verlag, Wiesbaden 2003.
[21] Pech A., Kolbitsch A., Zach F., *Decken,* Baukonstruktionen No. 5, Birkhäuser, Basel 2020.
[22] Stepan K. 2004 Vergleichende Untersuchungen von Deckensystemen des Stahlbeton-Skelettbaus, Dissertation. Technische Universität München.
[23] Pucher A., *Einflußfelder elastischer Platten = Influence surfaces of elastic plates,* Springer, Wien, New York 1964.
[24] Steffen S., Weidner S., Blandini L., Sobek W., *Using influence matrices as a design and analysis tool for adaptive truss and beam structures,* „Frontiers in Built Environment“ 2020 (6), p. 22–33.